A Tutorial on Thermal Sensors in the 200th Anniversary of the Seebeck Effect

F. Reverter

***Abstract*— Two noteworthy events associated to the physics of thermal sensors were demonstrated and announced in 1821, exactly two hundred years ago. The first event was the Seebeck effect, which led to the development of thermocouples. The second was the study of the thermal dependence of the resistivity of pure metals, which led to the design of resistance temperature detectors (RTD). Sensors' science and technology has experienced remarkable advances in the last decades, but these two types of thermal sensors, whose physics were announced 200 years ago, are still nowadays the main sensor technology in many industrial applications that require the measurement of extreme temperatures. In such a 200th anniversary, this tutorial aims to explain the operating principle, subtypes, input-output characteristic, limitations, and new trends under research of the four main types of thermal sensor: RTDs, thermistors, silicon sensors, and thermocouples. These are also compared with each other, highlighting the main advantages and disadvantages of each sensor technology.**

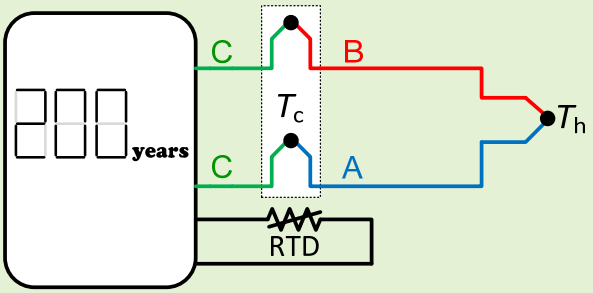

***Index Terms*— NTC, RTD, Seebeck effect, silicon sensor, smart sensor, temperature measurement, thermal sensor, thermistor, thermocouple.**

I. Introduction

SENSORS are the key element in any electronic instrumentation system applied to measurement and/or control. A sensor can be defined as a device that converts information from a given energy domain (such as thermal, mechanical, radiant/optical, chemical, or magnetic) to the electrical domain [1], as represented in Fig. 1. The sensor provides at its output an electrical signal, which is usually an analog signal, with information about the measurand. This electrical output signal can be in the form of a resistance, capacitance, inductance, voltage, current, or charge.

This tutorial focusses on thermal sensors, i.e. sensors that convert information from the thermal to the electrical domain, generally with an output signal in the form of a resistance, voltage or current. Temperature measurements are highly important in several fields: industrial, automotive, aerospace, medicine, consumer electronics, home appliances, research laboratories, among others. Temperature is a good indicator of the state/health of the object/subject under measurement. Thermal sensors are even embedded into integrated circuits to carry out an on-chip thermal monitoring that enable us to 1) identify hot spots caused by an extreme processing activity [2], and 2) obtain electrical figures-of-merit of other embedded circuits [3], [4]. The measurement of temperature is also employed to indirectly estimate other non-thermal magnitudes [5], for example: 1) the direction and speed of wind can be determined by means of a set of thermal sensors circularly distributed with a heater at the center [6], and 2) the mass flow can be measured through a couple of thermal sensors and an intermediate heater correctly aligned inside a pipeline. Another essential role of thermal sensors is to compensate for the thermal drifts of other non-thermal sensors, such as mechanical sensors [7].

Exactly two hundred years ago, in 1821, two highly remarkable events associated to the physics of thermal sensors were demonstrated and announced. On the one hand, the Seebeck effect related to thermocouples and, on the other hand, the temperature dependence of the resistivity of pure metals related to resistance temperature detectors (RTD). Although the great advances in sensors science and technology during the last decades, these two types of thermal sensor that were introduced 200 years ago are still widely employed, especially in industrial applications where extreme temperatures need to be monitored. To commemorate this 200th anniversary, a tutorial on thermal sensors is presented herein. The four main types of thermal sensors (RTDs, thermistors, silicon sensors, and thermocouples) are described and compared with each other. For each type of sensor, there is an explanation of the operating principle, subtypes, input-output (I/O) characteristic, limitations, and new trends under research. In addition, general considerations such as the self-heating error, protection and response time are also discussed.

Manuscript received Month xx, 2xxx; revised Month xx, xxxx; accepted Month x, xxxx. This work was supported in part by the Spanish Ministry of Economy and Competitiveness and the European Regional Development Fund under project TEC2016-76991-P.

Ferran Reverter is with the Department of Electronic Engineering, Universitat Politècnica de Catalunya – BarcelonaTech, Castelldefels (Barcelona), 08860, Spain (e-mail: ferran.reverter@upc.edu).

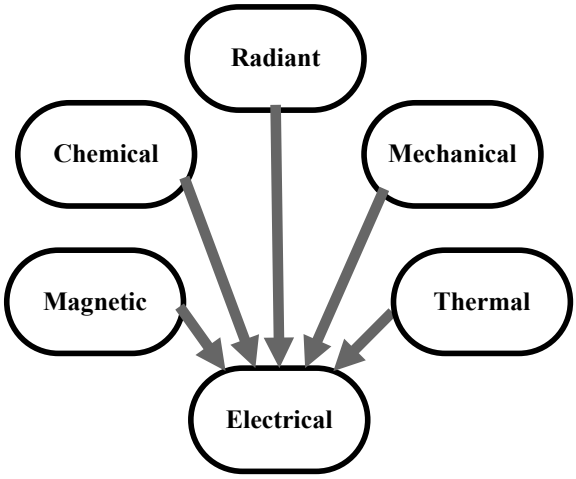

Fig. 1. Sensor acquiring information from different energy domains and converting it to the electrical domain.

II. Resistance Temperature Detector

The first type of thermal sensor discussed herein is the resistance temperature detector, so-called RTD. These RTD are usually made of platinum, thus being identified as PRTD. It is worthy to mention that the performance of these PRTD is standardized by the international standard IEC 60751 [8], [9].

A. Principle

The operating principle of RTDs rely on the fact that the resistivity (and, hence, the electrical resistance) of a pure metal increases with increasing temperature [10], which was announced by Sir Humphrey Davy in 1821. The physics behind this operating principle is that a temperature increase makes the thermal vibration of atoms higher and, hence, the electrons undergo a decrease of the mean time between collisions, thus increasing the resistivity of the metal.

As proposed by Sir William Siemens at the end of the 19th century, the metal most employed to manufacture RTD is platinum. This is due to the fact that platinum can withstand high temperatures with good stability and, in addition, it is a noble metal that shows an outstanding resistance to chemical attacks and pollution. Other metals employed, but less common, to manufacture RTDs are nickel and copper. The temperature input range for platinum-based RTD is from -200 to +850ºC, whereas for nickel- and copper-based counterparts is from -80 to +320ºC, and from -200 to +260ºC, respectively. The sensitivity of nickel-based RTDs is almost twice that offered by platinum-based RTD, but with less linearity.

B. Types

There are different criteria to classify the RTDs, for example, in terms of: a) the metal employed, as already indicated in the previous subsection, b) the manufacturing process, c) the accuracy provided, and d) the value of the sensor resistance at 0ºC. The last three criteria are discussed in more detail next.

In terms of manufacturing, two types of RTD can be distinguished: 1) wire-wound RTD, where a wire of platinum (or another metal) is wound in a substrate made of ceramic or glass; and 2) thin-film RTD, where a thin film of platinum is deposited in a non-conductive substrate. In both cases, the RTD is appropriately packaged or covered so as to protect the platinum. Thin-film RTDs are more compact in size, less expensive, and more robust to vibrations. However, these are more susceptible to the strain generated by temperature changes and, hence, provide a given accuracy in a narrower temperature range, with respect to the wire-wound counterparts.

TABLE I
Different Classes of RTD and their Properties according to IEC 60751

Class	Temperature range (ºC)		Tolerance (ºC) at 0ºC
	Wire wound	Thin film	
AA	[-50,+250]	[0,+150]	±0.10
A	[-100,+450]	[-30,+300]	±0.15
B	[-196,+600]	[-50,+500]	±0.30
C	[-196,+600]	[-50,+600]	±0.60

In terms of accuracy, the IEC 60751 distinguishes four classes of RTD: AA, A, B, and C, as summarized in Table I; the maximum error is specified by means of the tolerance, which assumes that the RTD has not been calibrated. Class-AA RTDs have the narrowest measurement range but the lowest tolerance, whereas Class-C RTDs show the widest measurement range but the highest tolerance. Class-A and class-B RTDs are the most employed, with a tolerance of ±0.15ºC and ±0.30ºC, respectively, at 0ºC. Note, however, that such a tolerance increases when the temperature moves away from 0ºC. Although PRTD can measure temperatures up to +850ºC, the range between the maximum temperature indicated in Table I and 850ºC is not covered by the standard.

In terms of the sensor resistance at 0ºC, PRTDs are available with a resistance of 50, 100, 200, 500, 1000, and 2000 Ω, but the most typical values are 100 and 1000 Ω. These two particular cases are known as Pt100 and Pt1000 offering a resistance of 100 Ω and 1000 Ω, respectively, at a temperature of 0ºC.

C. I/O characteristic

The relationship between the temperature (T, expressed in degrees Celsius) and the output resistance (R_t) of an RTD can be expressed as [8]:

$$R_t(T) = \begin{cases} R_0[1 + AT + BT^2 + C(T-100)T^3] \text{ for } T < 0ºC \\ R_0[1 + AT + BT^2] \text{ for } T > 0ºC \end{cases} \quad (1)$$

where R_0 is the resistance at 0ºC, and A, B, and C are the Callendar-Van Dusen coefficients provided by the sensor manufacturer. An example of how the resistance of a commercial Pt1000 depends on temperature is shown in Fig. 2 [11].

Since coefficient A is much higher than B and C (a factor of around 10^4 and 10^9, respectively), the polynomial in (1) can be simplified, in a narrow temperature range, as follows:

$$R_t(T) = R_0(1 + \alpha T) \quad (2)$$

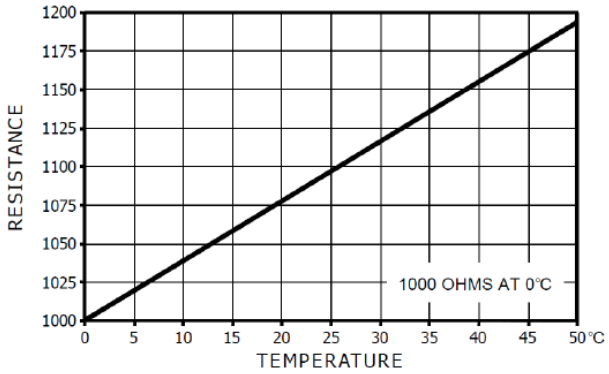

Fig. 2. Thermal dependence of the output resistance of a commercial Pt1000 [11].

where α is known as the (linear) temperature coefficient of the RTD, which is equal to 0.00385ºC^{-1} or a similar value in a PRTD. In a range of 50ºC, the error of the linear model in (2) with respect to (1) is approximately of 0.3ºC; note that this error corresponds only to the model simplification and does not include the tolerance indicated in Table I. The main advantage of applying a linear model, such as (2), is that the estimation of temperature (from the sensor output signal) carried out by the ensuing microprocessor or microcontroller is simpler and faster.

The thermal sensitivity of an RTD can be computed by making the derivative of (2) with respect to temperature, thus resulting in:

$$\frac{\partial R_t}{\partial T} = R_0 \alpha \qquad (3)$$

According to (3), the sensitivity is positive and constant. Assuming α = 0.00385 ºC^{-1}, the sensitivity equals 0.385 Ω/ºC for a Pt100, and 3.85 Ω/ºC for a Pt1000.

D. Limitation

The measurement of RTDs when these are remote (i.e. located at a certain distance from the read-out circuit [12]) and the value of R_0 is low (e.g. a Pt100) is not straightforward. In such conditions, the parasitic resistance of the interconnecting cables can cause a significant error in the temperature measurement. For example, the measurement of a Pt100 with an interconnecting cable whose resistance equals 1 Ω generates an error of 2.5ºC, which is much higher than the sensor tolerance.

In a two-wire measurement method (Fig. 3a), a current source (with a high output impedance) excites the RTD, thus resulting in a voltage drop that is measured with a circuit whose input impedance is high. However, such a technique is not recommended in the conditions indicated before because the parasitic resistance (R_c) of the cable is considered as a part of the sensor resistance. A solution to this problem is the four-wire measurement, also known as Kelvin resistance measurement, shown in Fig. 3b. Here, there is a couple of cables (C1 and C2) intended to inject the current, and another couple (C3 and C4) intended to measure the voltage drop exclusively between the terminals of the RTD. Since the circuit intended for the voltage measurement has a high input

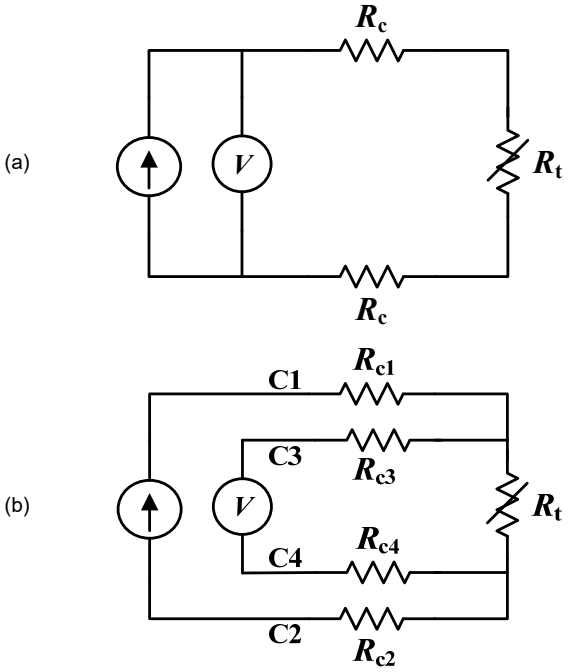

Fig. 3. (a) Two-wire and (b) four-wire measurement of an RTD,

impedance, the resistance of cables C3 and C4 (R_{c3} and R_{c4}, respectively) do not affect the reading. On the market, there are RTDs already prepared to carry out such a four-wire measurement, but these are more expensive.

E. New trends

The emergence of wearable electronics, artificial skins, and soft robotics is promoting the research on customizable RTD sensors, especially fabricated on a flexible substrate. In that sense, in the recent literature we can find Pt-based thin film flexible RTDs for temperatures up to 550ºC with a thermal hysteresis much lower than that obtained on a ceramic substrate [13]. Nickel-based flexible RTDs have also been recently suggested, with the corresponding benefits in terms of cost in comparison with the Pt-based counterparts. For instance, a new fabrication method based on laser digital pattering was proposed to manufacture Nickel-based RTDs with excellent repeatability in a temperature range up to 200ºC [14].

III. Thermistor

The second kind of thermal sensor explained next is the thermistor; this term is a contraction of the words *therm*ally sensitive res*istor*. These sensors offer a resistance at the output that changes with temperature, similarly to RTDs. The temperature input range of thermistors is narrower than that of RTDs, generally from -50 to +200ºC, although some specific models can measure up to 300ºC. The performance of thermistors is not standardized by any international standard.

A. Principle

Thermistors are resistive thermal sensors that rely on the fact that the resistivity (and, hence, the electrical resistance) of a semiconductor material depends on temperature. Such a

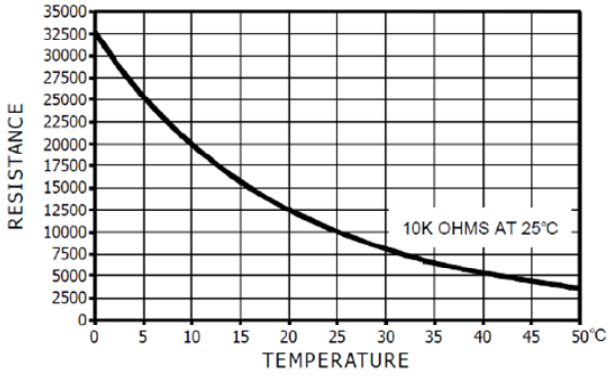

Fig. 4. Thermal dependence of the output resistance of a commercial NTC-thermistor [22].

physical phenomenon was reported for the first time by Michael Faraday in 1833 [15].

The physics behind the operating principle of thermistors depends on the semiconductor material employed in the fabrication. Depending on the material, an increase of temperature causes either an increase of the density of charge carriers or a decrease of the mean time between collisions, thus resulting in different types of I/O characteristic. This is reflected in the next subsections after classifying the thermistors in different subtypes.

B. Types

Thermistors can be classified in two types: 1) Positive Temperature Coefficient (PTC) thermistors, and 2) Negative Temperature Coefficient (NTC) thermistors. The output resistance of the former increases with increasing temperature, whereas that of the latter decreases.

There are two subtypes of PTC-thermistors [16]: linear (also known as *silistors*) and non-linear (also known as switching type). The former is made of silicon that is heavily doped with n-type impurities so that it assimilates conductor properties, thus resulting in a quite linear relationship in a narrow temperature range. The latter is fabricated using a polycrystalline ceramic material, such as barium titanate, that is normally highly resistive but is made semiconductive by the addition of dopants [17]. Its resistance shows an abrupt positive change above the Curie temperature, that generally ranges from −30ºC to +160ºC. For instance, in [18], the Curie point was set by controlling the contents of bismuth sodium titanate incorporated; the higher the contents, the higher the value of the Curie temperature. An international standard (IEC 60738-1) establishes the reliability tests of these switching-type PTC sensors.

NTC-thermistors are typically manufactured with sintered metal oxides, for example: ferric oxide with titanium doping [19], and nickel manganese oxide with lithium doping [20]. Using such semiconductor materials, a raising of the temperature increases the density of charge carriers, thus decreasing the resistivity and, hence, the resistance of the thermistor.

NTC-thermistors are more widely employed than PTC-thermistors, mainly because these are less expensive and offer a much better reproducibility. For this reason, the following subsections mostly focus on that type of thermistor.

C. I/O characteristic

The relation between the temperature (T, here expressed in degrees Kelvin) and the output resistance (R_t) of an NTC-thermistor can be accurately modelled by the Steinhart-Hart equation [21]:

$$\frac{1}{T} = A + B(\ln R_t) + C(\ln R_t)^3 \qquad (4)$$

where A, B, and C are curve-fitting constants. According to (4), the I/O characteristic is clearly non-linear. Figure 4 shows an example of how the resistance of a commercial NTC-thermistor depends on temperature [22].

For a narrow temperature range, it is quite common to apply a simpler model (so-called "β model") for NTC-thermistors, with the following resistance-temperature relationship:

$$R_t(T) = R_0 e^{\beta\left(\frac{1}{T}-\frac{1}{T_0}\right)} \qquad (5)$$

where R_0 is the resistance at the reference temperature (T_0), and β is a material-specific constant that is known as the *characteristic temperature*, which is quantified in kelvin. In a range of 50ºC, the error of the simplified model in (5) with respect to (4) is approximately of 0.3ºC. The reference temperature in (5) is typically 25ºC (298 K) and, for this reason, some manufacturers specify R_0 as R_{25} to emphasize that corresponds to 25ºC. On the other hand, β is sometimes specified as $\beta_{25/85}$ to indicate that this has been inferred from the resistance measurements at 25ºC and 85ºC. The value of R_0 generally ranges from 1 kΩ and 10 MΩ (for the case represented in Fig. 4, R_0 equals 10 kΩ), whereas β usually takes values between 2000 and 5500 K.

The derivative of (5) with respect to temperature provides the thermal sensitivity of an NTC-thermistor:

$$\frac{\partial R_t}{\partial T} = -\frac{\beta}{T^2} R_t \qquad (6)$$

which is negative and depends on temperature, as expected in a non-linear thermal sensor. For a typical NTC-thermistor with $R_0 = 10$ kΩ and $\beta = 4300$ K, the sensitivity resulting from (6) equals -484 Ω/K at 25ºC, which is much higher (at least, a factor of 100) than that obtained in RTDs.

As for "linear" PTC-thermistors, the resistance-temperature relationship can be modelled by a second-order polynomial [17]:

$$R_t(T) = R_0[1 + \alpha_1(T - T_0) + \alpha_2(T - T_0)^2] \qquad (7)$$

where R_0 is the resistance at the reference temperature (T_0), and α_1 and α_2 are the first-order and second-order coefficients, respectively. For example, for the KTY81-122 sensor (from NXP – Philips), $R_0 = 1$ kΩ, $T_0 = 25$ºC, $\alpha_1 = 0.007874$ ºC^{-1}, and $\alpha_2 = 1.874 \cdot 10^{-5}$ ºC^{-2} [17].

D. Limitation

The main limitation of NTC-thermistors is the non-linear I/O characteristic, as inferred from (4) and (5). There are different software and hardware techniques for improving the linearity. A software linearization can be carried out, for example, with a microcontroller including a lookup table and applying a linear interpolation. On the other hand, a hardware linearization can be easily performed by adding a resistor in parallel (R_p) or in series (R_s), as shown in Figs. 5a and 5b, respectively. In Fig. 5a, the equivalent resistance equals R_{eq}, whereas in Fig. 5b, a voltage divider is formed with an output voltage V_o.

The appropriate value of R_p in Fig. 5a can be determined by forcing, in the R_{eq}–T relationship, an inflection point at the central temperature (T_c) of the measurement range [23], thus resulting in:

$$R_p = \frac{\beta - 2T_c}{\beta + 2T_c} R_{t,c} \qquad (8)$$

where $R_{t,c}$ is the thermistor value at T_c. Fig. 6 shows an example of how the equivalent resistance depends on temperature when applying this linearization technique. In comparison to Fig. 4, the response is much more linear, but at the expense of degrading the sensitivity.

As for the linearization strategy shown in Fig. 5b, an optimal value of R_s can be determined by again forcing, in the V_o–T relationship, an inflection point at T_c. The result of that is an expression for R_s exactly equal to that provided for R_p in (8). Finally, note that R_p and R_s employed in Figs. 5a and 5b, respectively, should have a low temperature coefficient.

E. New trends

New materials for the fabrication of NTC-thermistors, replacing the conventional sintered metal oxides, are nowadays studied and proposed. The feasibility of employing liquid crystal materials to develop NTC-thermistors with an interdigital electrode structure was demonstrated in [24]. The performance of those thermistors followed the Steinhart-Hart equation and showed a good long-term stability. Recent literature also suggests the fabrication of polymer-based flexible NTC-thermistors [25], which can be cured at low temperatures; there is no need of high sintering temperatures (i.e., 1200-1300ºC) as occurs in thermistors based on metal oxides. Such thermistors offered a satisfactory response under high-humidity conditions, which was one of the main limitations of the previous similar flexible designs.

IV. Silicon Sensor

The third type of thermal sensor described herein is the silicon sensor, also so-called PN junction, integrated, monolithic, semiconductor, or solid-state thermal sensor. Although the term *silicon sensor* is the most commonly employed one in the literature and also along this tutorial, the term *PN junction sensor* [17] is, in the opinion of this author, the most appropriate. Using the first term, it could seem that the silistors discussed in Section III.B, which are made of silicon, belong to the category presented herein, but they actually do not. Note also that not all the integrated thermal sensors (e.g. AD22100 from Analog Devices) rely on the operating principle explained here.

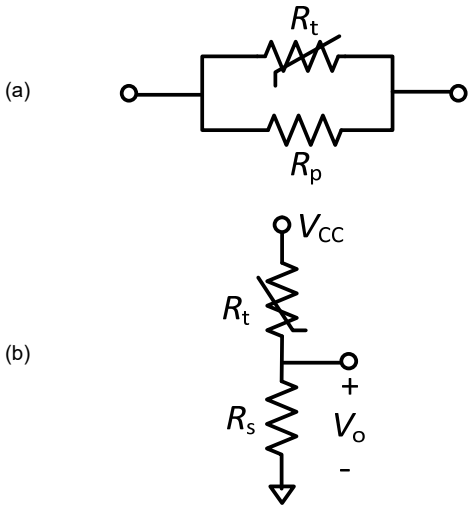

Fig. 5. Linearization of an NTC-thermistor using (a) a resistance in parallel, and (b) a resistance in series in a voltage divider.

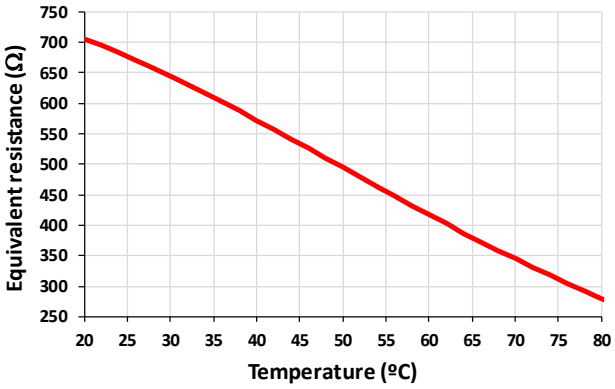

Fig. 6. Example of the resulting equivalent resistance in Fig. 5a with an inflection point at the center of the measurement range (50ºC).

The electrical output signal of these silicon thermal sensors is generally a voltage or a current that changes with temperature. The performance of these sensors is not standardized by any international standard, as it also occurs for the thermistors presented in Section III.

A. Principle

The essence behind the operating principle of silicon sensors, which was introduced in 1960s, is that the forward voltage of a semiconductor PN junction depends on temperature, due to the thermal dependence of both the saturation current (I_s) and the thermal voltage ($V_T = k \cdot T/q$). Note that I_s depends on several temperature-dependent parameters, such as the intrinsic carrier concentration, effective hole mobility, and Gummel number [26]. Actually, a simple diode can be employed as a thermal sensor by measuring the forward voltage at a constant forward current [27]. Nevertheless, diodes provide low accuracy due to the non-ideality factor in the I-V characteristic caused by the recombination of electron-hole pairs in the depletion region

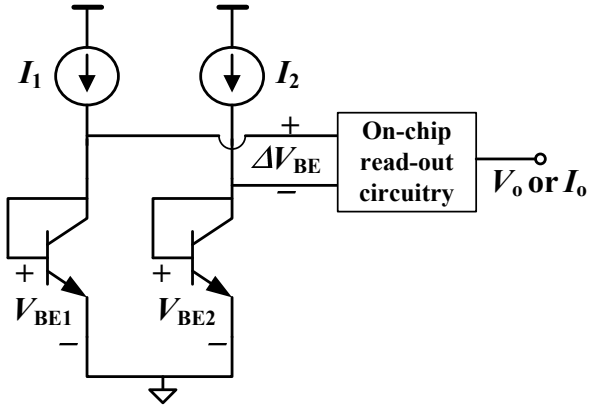

Fig. 7. Silicon thermal sensor based on two bipolar transistors biased at different currents.

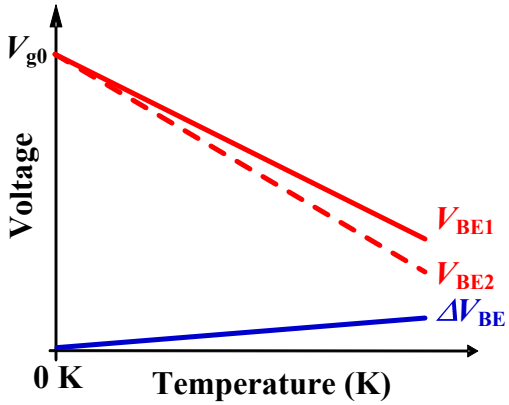

Fig. 8. Temperature dependence of the V_{BE} of the two bipolar transistors shown in Fig. 7, and the resulting ΔV_{BE}; V_{go} is the extrapolated band-gap voltage at 0 K.

[26]. A more accurate measurement can be carried out using as a sensing element the base-emitter junction of a bipolar transistor [28], which is biased at a constant current and in a diode-connected topology (i.e. the base and collector terminals are short-circuited). In such conditions, the base-emitter voltage (V_{BE}) provides information about the temperature with a sensitivity of around –2 mV/ºC. However, this thermal sensitivity depends on the chip fabrication process. A spread of the sensitivity of around 2% has been reported [29], thus resulting in an error up to 4ºC at the high end of the temperature range. In addition, V_{BE} is quite sensitive to the mechanical stress generated by the mismatch in the thermal expansion coefficient of the different materials involved [30]. This generates long-term drifts and a poor repeatability.

Considering the previous limitations, the information about temperature is generally embedded in the difference (ΔV_{BE}) between the base-emitter voltage of two bipolar transistors that are at the same temperature but operate at different current densities, as shown in Fig. 7 [29]. Such a different current density can be achieved using transistors of the same dimensions but biased at different currents (I_1 and I_2 in Fig. 7), transistors of different dimensions biased at the same current, or changing both dimensions and bias currents. The resulting ΔV_{BE} is Proportional To Absolute Temperature (PTAT), as represented in Fig. 8, and is given by [26]:

$$\Delta V_{BE} = V_T \ln(p \cdot r) \tag{9}$$

where p is the bias-current ratio, and r is the emitter-area ratio. For typical values of $p \cdot r$ between 3 and 16, the thermal sensitivity of ΔV_{BE} is in the order of 100-250 µV/ºC. This temperature-dependent voltage is then connected to on-chip read-out circuitry with several functions [26]: amplification, offset cancellation, analog-to-digital (ADC) conversion, among others. Note that in CMOS technology, which is the most employed for the design of integrated circuits (IC), there are bipolar transistors available that can be employed as a sensing element [29].

Although less common, silicon thermal sensors can also rely on MOSFET transistors [31], [32], instead of bipolar transistors. In such a case, a diode-connected MOSFET biased with a constant current provides a gate-source voltage (V_{GS}), or a difference of V_{GS} (ΔV_{GS}) when using two diode-connected MOSFETs, that depends on temperature; this is due to the thermal dependence of both the carriers mobility and the threshold voltage. In comparison with the bipolar case, the resulting thermal sensitivity can be higher, but also the dependence on the fabrication process. PTAT topologies based on MOSFETs operating in weak inversion have also been proposed [33], with the corresponding advantages in terms of current consumption.

B. Types

The topology shown in Fig. 7, or a very similar one, can be considered as the core of most commercial silicon thermal sensors. However, these sensors can have different types of on-chip read-out circuitry and, hence, ΔV_{BE} is processed in different ways, thus providing different types of output signal with information about the temperature. Therefore, from the user's point of view, the different subtypes of silicon sensors can be classified according to the output signal. Typically, the output signal has been either a voltage (V_o) or a current (I_o) that linearly increases with increasing temperature [21]. In addition, such an output voltage or current is usually adjusted in the Kelvin scale or in the Celsius scale so that it has a typical value of zero at 0 K or at 0ºC, respectively.

On the semiconductor market, there are also silicon thermal sensors with a time-modulated output signal, for example: a signal whose period or frequency depends on temperature. Silicon thermal sensors with a digital output signal are also available. In such a case, the sensor chip includes an ADC and the corresponding series communication interface blocks (e.g. I²C or SPI). These chips including the sensing element shown in Fig. 7 together with so many other electronic blocks to facilitate the output reading and communication belong to the category of *smart sensors* [1].

C. I/O characteristic

The I/O characteristic of silicon sensors providing an output voltage can be expressed, in a first approximation, as

$$V_o(T) = V_{off} + S(T - T_0) \tag{10}$$

where V_{off} is the output voltage at the reference temperature (T_0), S is the thermal sensitivity in mV/K or mV/ºC, and T is the temperature that can be expressed in K or ºC. Table II

TABLE II
COMMERCIAL SILICON THERMAL SENSORS PROVING AN OUTPUT VOLTAGE

Model	T_0	V_{off}	S
LM35 [a]	0ºC	0 V	10 mV/ºC
LM335 [a]	0 K	0 V	10 mV/K
TMP37 [b]	0ºC	0 V	20 mV/ºC
TMP36 [b]	0ºC	0.5 V	10 mV/ºC

[a] From Texas Instruments
[b] From Analog Devices

shows different commercial sensors that follow (10) and the corresponding value of the variables involved. In those examples, only the LM335 is adjusted in the Kelvin scale.

For silicon sensors providing an output current, the I/O characteristic can be written as:

$$I_o(T) = I_{off} + S(T - T_0) \qquad (11)$$

where I_{off} is the output current at T_0, S is the thermal sensitivity in µA/K or µA/ºC, and T is the temperature (in K or ºC). Many commercial sensors are adjusted in the Kelvin scale following (11) with T_0 = 0 K, I_{off} = 0 A, and S = 1 µA/K. This is the case, for example, of AD590 and TMP17 from Analog Devices, and ISL71590 from Intersil. The latter is a special thermal sensor especially designed for aerospace applications since it has a robust response in front of high radiation levels; it belongs to the category of *rad-hard* electronics.

In (10) and (11), it is assumed that the I/O characteristic of silicon sensors is completely linear, but actually it is not. Commercial silicon sensors can undergo a non-linearity error that ranges from ±0.5 to ±1.5ºC.

D. Limitation

The main limitation of silicon thermal sensors is that their input temperature range is quite narrow, from –50 to +150ºC in the best of the scenarios. Note, however, that this limited temperature range includes most of the activities of the human being and, for this reason, silicon sensors are still widely employed.

The previous limitation is not specific for silicon thermal sensors, but it is applicable to any IC manufactured in standard CMOS technology, which is the most employed nowadays. The designers of ICs have powerful simulation tools including complex electrical models of the transistors, but these models are valid within a limited temperature range. For temperatures lower than –50ºC or higher than +150ºC, the available electrical models are not accurate enough. For instance, for temperatures higher than 150ºC, the leakage current of the parasitic PN junctions is very high but not well-characterized in the electrical models. Without reliable simulation results, the manufacturing of an IC is not recommended.

E. New trends

In the recent literature, many low-area, low-power silicon thermal sensors have been proposed and developed. Note that these sensors are widely employed for the on-chip thermal management of integrated circuits and, hence, the area and power overload caused by the thermal sensor(s) should be as low as possible [34]. For instance, a silicon sensor based on MOSFET transistors operating in weak inversion with a power consumption of tens of nW was suggested in [35]. This sensor, however, had a limited temperature range from –20 to +80ºC and an inaccuracy up to –2.5ºC. Another silicon sensor based on bipolar transistors with a wider temperature range (from –40 to +125ºC) and a lower inaccuracy (±0.5ºC), but a higher power consumption (tens of µW) was recently proposed in [36]. Both previous designs occupy a small layout area (i.e., lower than 0.1 mm^2) and offer a time-modulated output signal.

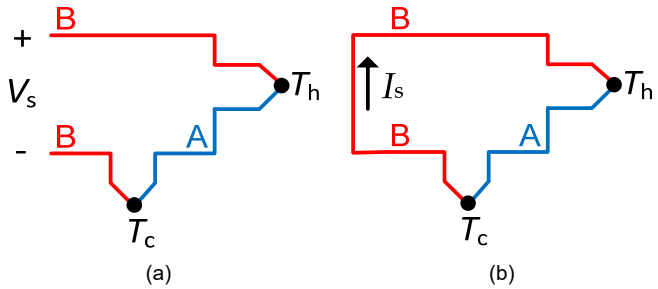

Fig. 9. Operating principle of thermocouples according to the Seebeck effect.

V. THERMOCOUPLE

The last type of thermal sensor explained in detail is the thermocouple. This provides an output voltage that depends on temperature, as in the silicon sensors. However, in comparison to silicon sensors, thermocouples offer a much wider temperature range, but a lower value of the thermal sensitivity.

Thermocouples belong to the category of *self-generating* sensors, since they are able to provide an output signal with information about the measurand (here, the temperature) without requiring any external power. This is not the case for the thermal sensors explained in the previous sections. For instance, a silicon sensor outputs a signal with information about temperature provided that this is well supplied, otherwise the output signal is zero.

A. Principle

Thermocouples rely on the Seebeck effect, which was demonstrated in 1821 by Thomas Seebeck [37]. According to this thermoelectric effect, a voltage difference (V_s) is generated across the terminals of an open circuit made up of a pair of dissimilar metals or alloys (A and B) whose two junctions are held at different temperatures (T_h and T_c), as shown in Fig. 9a. The generated voltage, so-called Seebeck voltage, depends on the metals employed and also on the thermal difference $T_h - T_c$, but does not depend on the distribution of temperature along the metals between the junctions. If the thermoelectric circuit in Fig. 9a is closed, then a current (I_s) flows through the metals, as represented in Fig. 9b.

The junction in Fig. 9a at T_h is so-called the hot or measuring junction, whereas that at T_c, the cold or reference junction. In most applications, T_h is the temperature to be measured, whereas T_c is at a known temperature, which can be constant or not. During the characterization of thermocouples

°C	0	1	2	3	4	5	6	7	8	9	10
0	0.000	0.039	0.078	0.117	0.156	0.195	0.234	0.273	0.312	0.352	0.391
10	0.391	0.431	0.470	0.510	0.549	0.589	0.629	0.669	0.709	0.749	0.790
20	0.790	0.830	0.870	0.911	0.951	0.992	1.033	1.074	1.114	1.155	1.196
30	1.196	1.238	1.279	1.320	1.362	1.403	1.445	1.486	1.528	1.570	1.612
40	1.612	1.654	1.696	1.738	1.780	1.823	1.865	1.908	1.950	1.993	2.036
50	2.036	2.079	2.122	2.165	2.208	2.251	2.294	2.338	2.381	2.425	2.468
60	2.468	2.512	2.556	2.600	2.643	2.687	2.732	2.776	2.820	2.864	2.909
70	2.909	2.953	2.998	3.043	3.087	3.132	3.177	3.222	3.267	3.312	3.358
80	3.358	3.403	3.448	3.494	3.539	3.585	3.631	3.677	3.722	3.768	3.814
90	3.814	3.860	3.907	3.953	3.999	4.046	4.092	4.138	4.185	4.232	4.279

Fig. 10. Characteristic table of a type T thermocouple that provides the output voltage (V_s in Fig. 9a) in mV at intervals of 1ºC, assuming T_c = 0ºC.

TABLE III
DIFFERENT TYPES OF STANDARD THERMOCOUPLE AND THEIR MAIN FEATURES

Type	Metal or alloy +	Metal or alloy -	Sensitivity (μV/ºC)	Temperature range (ºC)
T	Cu	Cu - Ni	38.7 (at 0ºC)	[-270,+400]
J	Fe	Cu - Ni	50.4 (at 0ºC)	[-210,+1200] [a]
K	Ni - Cr	Ni - Al	39.4 (at 0ºC)	[-270,+1300]
E	Ni - Cr	Cu - Ni	58.7 (at 0ºC)	[-270,+1000]
R	Pt – 13% Rh	Pt	11.4 (at 600ºC)	[-50,+1768]
S	Pt – 10% Rh	Pt	10.2 (at 600ºC)	[-50,+1768]

[a] But recommended up to 760ºC

in calibration laboratories, T_c is forced at 0ºC by means of an ice bath and V_s is measured at different values of T_h. This is then reported in tables like the one provided in Fig. 10, which corresponds to a type T thermocouple.

B. Types

There are different types of thermocouple depending on the metals or alloys employed. The features of standard thermocouples, also so-called letter-designated thermocouples, are standardized by international standards, such as IEC 60584 [38] and NIST ITS-90. However, the Seebeck effect is also applicable to other combinations of metals (or alloys) non-specified in these standards. For example, thermocouples can be implemented with materials commonly employed in CMOS technology, thus resulting in an on-chip non-standard thermocouple [39].

If we focus on the standard thermocouples, these can be classified into two different construction types: base metal thermocouples (types J, K, N, E, and T) and noble metal thermocouples (types R, S, and B). The former ones are cheaper, but less accurate and with a narrower temperature range. For the measurement of very high values of temperature (up to 2300ºC), there is a third subtype of thermocouples made of tungsten (types C and A), but these have to be used in a chemically-inert environment. Table III summarizes the features of some of these thermocouples, indicating the metals (or alloys) involved, the thermal sensitivity at a given temperature and the input temperature range [38]. This temperature range is mainly determined by the corrosion and oxidation affecting the metals or alloys of the thermocouple.

In comparison with the thermal sensors explained before, thermocouples can measure higher values of temperature but with a lower thermal sensitivity. Higher values of sensitivity

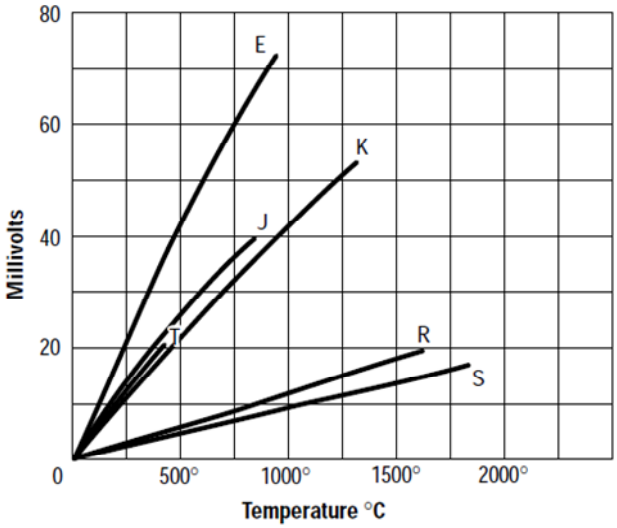

Fig. 11. Thermal dependence of the output voltage for different types of standard thermocouples [21].

can be obtained by connecting several thermocouples in series [39]. Such a sensor topology is known in the literature as *thermopile*, which is employed, for instance, as a thermal radiation sensor.

C. I/O characteristic

The relationship between the temperature (T, expressed in degrees Celsius, which corresponds to T_h in Fig. 9) and the output voltage (V_s, quantified in μV) of a thermocouple can be written using the following polynomial [38]:

$$V_s(T) = \sum_{i=0}^{n} a_i \cdot T^i \qquad (12)$$

where a_i is the i^{th} coefficient of the polynomial, and n is the order of the polynomial. The values of a_i and n depend on the type of thermocouple and also on the temperature range, and these are tabulated for standard thermocouples in [38] assuming the reference junction at 0ºC. The values of voltage resulting from (12) equal those given in characteristic tables like in Fig. 10. An example of how the output voltage depends on temperature is shown in Fig. 11 for the same standard thermocouples specified before in Table III [21].

Taking into account that a_1 is much higher than the other coefficients (at least, a factor of 100) and that a_0 equals zero when the temperature range includes 0ºC, the polynomial in (12) can be simplified, in a narrow temperature range, as follows:

$$V_s(T) = S \cdot T \qquad (13)$$

where S is known as the Seebeck coefficient or the sensitivity of the thermocouple at 0ºC, and corresponds to the coefficient a_1 in (12). For example, in a temperature range of 50ºC, the error of the linear model in (13) with respect to (12) is around 2ºC in a type T thermocouple.

D. Limitation

In the previous subsections, it is assumed that the reference

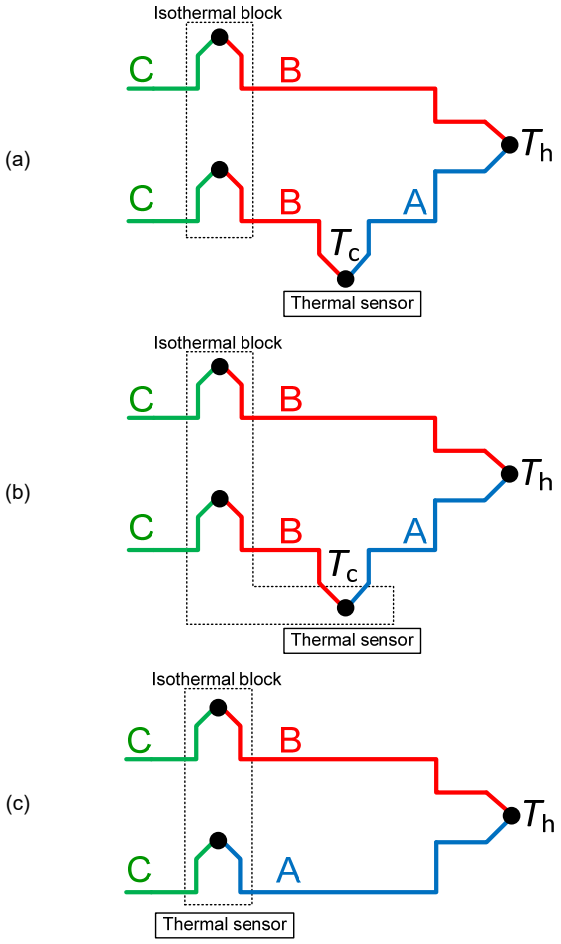

Fig. 12. Thermocouple including an isothermal block to cancel the thermoelectric effects of the parasitic junctions, and an additional thermal sensor for the cold-junction compensation.

or cold junction of the thermocouple is at 0ºC. Although this is practicable in calibration labs through an ice bath, it is not in low-cost, industrial applications. In such cases, instead of forcing the cold junction at a known and constant temperature, an additional thermal sensor measures T_c to carry out a *cold-junction compensation*. Then, thanks to the application of the *law of intermediate temperatures* of thermocouples, the methodology to determine T_h is the following [40]:

1) T_c is measured via the additional thermal sensor.

2) T_c is converted to a voltage $V_{s,c}$ using either a characteristic table like the one in Fig. 10 or a polynomial such as (12).

3) $V_{s,c}$ is added to the measured output voltage (V_s) in Fig. 9a, thus resulting in $V_{s,new}$, which would be the actual output voltage if T_c was 0ºC.

4) $V_{s,new}$ is then converted to T_h using again either a characteristic table or a polynomial.

Any of the three previous types of thermal sensor (RTD, thermistor, or silicon sensor) can act as the required additional thermal sensor. Note, however, that none of these types can measure extreme values of temperature and, hence, the use of a thermocouple together with this additional thermal sensor is mandatory in some applications.

Another limitation of thermocouples are the parasitic junctions that appear when these are connected to the measuring instrument. This is represented in Fig. 12a via the junctions C-B, where C is the metal at the input of the instrument, which is usually copper. In order to cancel the thermoelectric effects of these two parasitic junctions, an isothermal block (which is a special connector for thermocouples that acts as a thermal short-circuit) is required to ensure that these two are at the same temperature.

Let us assume now that the isothermal block also includes the cold junction, as represented in Fig. 12b. At the bottom side of the thermocouple, the two junctions of the three metals involved (A, B, and C) are at the same temperature. In such conditions and according to the *law of intermediate metals* [21], the presence of metal B does not alter the generated voltage. Therefore, the thermoelectric circuit in Fig. 12b can be simplified to that in Fig. 12c, where the temperature of the isothermal block acts as the temperature of the cold junction to be compensated for.

E. New trends

The study of new materials for the fabrication of thermocouples is nowadays under investigation. One of the current challenges is the design of single-material thermocouples, which usually consist of a U-shaped structure with a narrow and a wide leg joined at the temperature sensing end. For example, this concept has been demonstrated using stripes of graphene with a sensitivity of 39 µV/K [41]. Single-material thermocouples have also been fabricated using low-cost graphite coming from pencils of different grade, thus resulting in a sensitivity of 7 µV/K [42]. Another topic under research is the design of thermocouples for smart textiles [43]. These thermocouples have to combine the flexibility and light weight of textiles with the conductive property of the conductor materials.

VI. Other Considerations

A. Self-heating

The thermal sensors that require an external power to operate (i.e. RTDs, thermistors, and silicon sensors) can undergo an error due to self-heating. These sensors dissipate power (P_d) by Joule effect and, in consequence, the temperature detected (T_s) can be higher than the actual temperature of the medium (T_m) to be sensed. This effect can be modelled as follows:

$$T_s = T_m + \Delta T \tag{14}$$

where ΔT is the increment of temperature (and, hence, an error) caused by the self-heating. Of course, this error must lower than the maximum error allowed in the measurement system under design.

As for RTDs and thermistors, (14) is usually written as

$$T_s = T_m + \frac{P_d}{\delta} \tag{15}$$

where δ is the heat dissipation factor quantified in mW/K (or mW/ºC). This factor takes values of units or tens of mW/K and depends, among others, on the operating environment of

TABLE IV
COMPARISON BETWEEN THE DIFFERENT TYPES OF THERMAL SENSOR

Feature	PRTD	NTC-Thermistor	Silicon	Thermo-couple
Temp. range	H/M	M/L	**L**	**H**
Accuracy	**H**	L	M	H/M
Linearity	H	**L**	H/M	M
Sensitivity	M	**H**	H/M	**L**
Read-out circuit complexity	M	M	**L** [a]	**H**
CMOS compatibility	No	No	**Yes**	Yes [b]
Self-heating	Yes	Yes	Yes	No
Cost	**H**	L	L	M/H [c]

Abbreviations: L: Low; M: Medium; H: High
[a] From the user's point of view.
[b] But without being a standard type.
[c] It depends on the type of metal (base or noble) employed.

the sensor. For example, in still air conditions, the resulting value of δ is low, which means that a low value of dissipated power causes a significant increase of temperature. Generally, the manufacturer of the sensor provides different values of δ corresponding to different operating environments.

On the other hand, for silicon sensors, (14) is typically expressed as

$$T_s = T_m + P_d R_{\theta jA} \tag{16}$$

where $R_{\theta jA}$ is the junction-to-ambient thermal resistance, which takes values of tens or hundreds of K/W (or ºC/W). As before, this thermal resistance depends on the operating conditions and also on the package of the chip. Actually, the factors $R_{\theta jA}$ in (16) and δ in (15) are equivalent, but the former is the reciprocal of the latter.

B. Protection and response time

Some thermal sensors explained before (mainly RTDs and thermocouples, but also thermistors) may require a protection sheath if the measuring environment is aggressive. This sheath protects the sensor from contamination and physical damage caused by the materials, liquids or other environment elements [44]. Common sheath materials are iron, steel, stainless steel, ceramics, and porcelain. Note that it is difficult to distinguish the type of thermal sensor when this is inserted into a sheath, although the output signal provided is completely different.

The response time depends on either the sensing element is directly exposed to the medium or it is inserted into a sheath. When the sensor is not protected, the thermal mass is low and, hence, the sensor output signal quickly reacts to any temperature change. On the contrary, if the sensor is inserted into a sheath, the thermal mass is higher and the response time is longer. The overall response time also depends on the sheath material and diameter, and the surrounding medium. In order to quantify this response time, it is generally assumed that the sensor behaves as a first-order system with a certain thermal time constant [17]. For applications that require a fast response time (say, less than 1 s), it is advisable to employ an unprotected thermocouple or a small thermistor.

VII. COMPARISON

A comparison of the main features of the four types of thermal sensor explained before is summarized in Table IV. The main advantage(s) of each type is highlighted in blue, whereas the main drawback(s), in red. As inferred from Table IV, the ideal thermal sensor does not exist, but each type offers pros and cons. The most appropriate thermal sensor for a given application is that one that better adapts to the technical and economic requirements.

In relation to the read-out circuit complexity, note that measurement of a thermocouple involves the measurement of an additional thermal sensor for the cold-junction compensation. Therefore, the overall read-out circuit is more complex since it requires two analog inputs and a multiplexer before the ensuing amplifier and ADC [45]. In addition, thermocouples offer a low-amplitude output signal and, hence, any non-ideality of the circuit (e.g. the input offset voltage of the required OpAmps) can be more critical. Accordingly, the design of the specific amplifier circuit intended for the thermocouple is also more complex than for the other types of thermal sensor.

The four types of thermal sensor described before can be employed in a multitude of different scenarios, but next a summary of their main applications is provided. PRTDs and thermocouples are mostly used in industrial and aerospace applications. For example, PRTDs are quite common in the food and pharmaceutical industries that require high-accuracy thermal measurements, whereas thermocouples are more usual in extreme operating conditions, such as the thermal measurement of aircraft exhaust gases. NTC-thermistors are mainly employed in household appliances, heating, ventilation and air conditioning (HVAC) systems, and in the automotive sector. Finally, the main application field of silicon sensors is the thermal compensation (e.g. of mechanical sensors) and the thermal management (e.g. of a central processing unit, CPU) of other electronic components.

VIII. CONCLUSION

With the aim of helping the reader to become familiar with and/or improve his/her knowledge about thermal sensors, a tutorial on them has been presented. For the four main types of thermal sensor (i.e. RTDs, thermistors, silicon sensors, and thermocouples), this tutorial has explained their operating principle, subtypes, input-output characteristic, limitations, and new trends under research. In addition, their features have been compared with each other, highlighting the main advantages and disadvantages of each sensor technology.

REFERENCES

[1] J. H. Huijsing, "Smart sensor systems: Why? Where? How?," in *Smart Sensor Systems*, G. C. M. Meijer (Ed.), Chichester, UK: Wiley, 2008, ch. 1, pp 1-21.
[2] T. Yang, S. Kim, P. R. Kinget, and M. Seok, "Compact and supply-voltage-scalable temperature sensors for dense on-chip thermal

monitoring," *IEEE J. Solid-State Circuits*, vol. 50, no. 11, pp. 2773–2785, Oct. 2015.
[3] F. Reverter *et al.*, "MOSFET dynamic thermal sensor for IC testing applications," *Sens. Actuators A Phys.*, vol. 242, pp. 195–202, May 2016.
[4] F. Reverter *et al.*, "Single-MOSFET DC thermal sensor for RF-amplifier central frequency extraction," *Sens. Actuators A Phys.*, vol. 264, pp. 157–164, Sep. 2017.
[5] G. C. M. Meijer and A. W. van Herwaarden, *Thermal sensors*. Delft, The Netherlands: Delft University of Technology publications, 1992.
[6] K. A. A. Makinwa, "Flow sensing with thermal sigma-delta modulators," Ph.D. dissertation, Delft University of Technology, Delft, The Netherlands, 2004.
[7] F. Reverter, G. Horak, V. Bilas, and M. Gasulla, "Novel and low-cost temperature compensation technique for piezoresistive pressure sensors," in *Proc. XIX IMEKO World Congress*, Lisbon, Portugal, 2009, pp. 2084-2087.
[8] *Industrial platinum resistance thermometers and platinum temperature sensors*, IEC 60751, 2008.
[9] J. P. Tavener, "Changes to the International Standard for Industrial PRT's (IEC 60751 Ed.2 2008)," in *Proc. Test and Meas. Conf.,* Drakensberg, South Africa, 2010, pp. 1-8.
[10] R. Pallàs-Areny and J. G. Webster, *Sensors and Signal Conditioning*. New York: John Wiley & Sons, 2001.
[11] Honeywell International Inc., C7080A3100 datasheet.
[12] P. R. Nagarajan, B. George, and V. J. Kumar, "Improved single-element resistive sensor-to-microcontroller interface," *IEEE Trans. Instrum. Meas.*, vol. 66, no. 10, pp. 2736-2744, Oct. 2017.
[13] L. Shao *et al.*, "Pt thin-film resistance temperature detector on flexible Hastelloy tapes," *Vacuum*, vol. 184, 109966, 2021.
[14] V. B. Nam and D. Lee, "Evaluation of Ni-based flexible resistance temperature detectors fabricated by laser digital pattering," *Nanomaterials*, vol. 11, 576, 2021.
[15] M. Faraday, *Experimental Researches in Electricity.* London: Richard and John Edward Taylor, 1839.
[16] Texas Instruments, "Temperature sensing with thermistors," Report SLAY054, 2020.
[17] J. Fraden, *Handbook of Modern Sensors. Physics, Designs, and Applications*. New York: Springer, 2004.
[18] W. Huo and Y. Qu, "Effects of $Bi_{1/2}Na_{1/2}TiO_3$ on the Curie temperature and the PTC effects of $BaTiO_3$-based positive temperature coefficient ceramics," *Sens. Actuators A Phys.*, vol. 128, pp. 265–269, 2006.
[19] Wiendartun and D. G. Syarif, "The effect of MnO_2 content and sintering atmosphere on the electrical properties of iron titanium oxide NTC thermistors using yarosite," *Journal of Physics: Conference Series*, vol. 812, 012120, 2017.
[20] M. L. Martínez Sarrión and M. Morales, "Preparation and characterization of NTC thermistors: nickel manganites doped with lithium," *J. Am. Ceram. Soc.*, vol. 78, no. 4, pp. 915–921, 1995.
[21] Hewlett Packard, "Practical Temperature Measurements," App. Note 290, 1997.
[22] Honeywell International Inc., C7080A1100 datasheet.
[23] F. Reverter, "A microcontroller-based interface circuit for non-linear resistive sensors," *Meas. Sci. Technol.*, vol. 32, 027001 (4pp), 2021.
[24] J. Sun *et al.*, "Thermistor-based nematic liquid crystal IM95100-000," *IEEE Trans. Electron Devices* (early access).
[25] B. B. Maskey *et al.*, "Proving the robustness of a PEDOT:PSS-based thermistor via functionalized graphene oxide-poly(vinylidene fluoride) composite encapsulation for food logistics," *RSC Adv.*, vol. 10, pp. 12407–12414, 2020.
[26] M. Pertijs, "Precision temperature sensors in CMOS technology," Ph.D. dissertation, Delft University of Technology, Delft, The Netherlands, 2005.
[27] M. Mansoor, I. Haneef, S. Akhtar, A. De Luca, and F. Udrea, "Silicon diode temperature sensors—A review of applications," *Sens. Actuators A Phys.*, vol. 232, pp. 63-74, 2015.
[28] G. C. M. Meijer, "Thermal sensors based on transistors," *Sens. Actuators*, vol. 10, pp. 103-125, 1986.
[29] M. A. P. Pertijs, G. C. M. Meijer, and J. H. Huijsing, "Precision temperature measurement using CMOS substrate PNP transistors," *IEEE Sens. J.*, vol. 4, no. 3, pp. 294-300, June 2004.
[30] G. C. M. Meijer, G. Wang, and F. Fruett, "Temperature sensors and voltage references implemented in CMOS technology," *IEEE Sens. J.*, vol. 1, no. 3, pp. 225–234, Oct. 2001.
[31] I. M. Filanovsky and A. Allam, "Mutual compensation of mobility and threshold voltage temperature effects with applications in CMOS circuits," *IEEE Trans. Circuits and Systems-I*, vol. 48, no. 7, pp. 876-884, July 2001.
[32] F. Reverter and J. Altet, "MOSFET temperature sensors for on-chip thermal testing," *Sens. Actuators A Phys.,* vol. 203, pp. 234-240, 2013.
[33] A. Kölling, F. Bak, P. Bergveld, and E. Seevinck, "Design of a CMOS temperature sensor with current output," *Sens. Actuators*, vol. 22, pp. 645–649, 1990.
[34] J. Shor, "Compact thermal sensors for dense CPU thermal monitoring and regulation: A review," *IEEE Sens. J.*, vol. 21, no. 11, pp. 12774–12788, June 2021.
[35] A. Azam, Z. Bai, and J. S. Walling, "An ultra-low power CMOS integrated pulse-width modulated temperature sensor," *IEEE Sens. J.*, vol. 21, no. 2, pp. 1294–1304, Jan. 2021.
[36] Z. Huang *et al.* "A BJT-based CMOS temperature sensor with duty-cycle-modulated output and ±0.54ºC (3σ) inaccuracy from -40ºC to 125ºC," *IEEE Trans. Circuits Syst. II Express Briefs* (early access).
[37] T. J. Seebeck, "Ueber die magnetische Polarisation der Metalle und Erze durch Temperaturdifferenz," *Ann. Phys.*, vol. 82, no. 3, pp. 253–286, Jan. 1826.
[38] *Thermocouples – Part 1: EMF specifications and tolerances*, IEC 60584-1, 2013.
[39] E. Aldrete-Vidrio, D. Mateo, and J. Altet, "Differential temperature sensors fully compatible with a 0.35-µm CMOS process," *IEEE Trans. Components and Packaging Technologies*, vol. 30, no. 4, pp. 618–626, Dec. 2007.
[40] National Instruments, "Measuring temperature with thermocouples – a tutorial," App. Note 043, 1996.
[41] A. Harzheim, F. Könemann, B. Gotsmann, H. van der Zant, and P. Gehring, "Single-material graphene thermocouples," *Adv. Funct. Mater.*, vol. 30, 2000574, 2020.
[42] R. Mulla and C. W. Dunnill, "Single material thermocouples from graphite traces: fabricating extremely simple and low cost thermal sensors," *Carbon Trends* (early access).
[43] W. Root, T. Bechtold, and T. Pham, "Textile-integrated thermocouples for temperature measurement," *Materials*, vol. 13, 626, 2020.
[44] Keithley Instruments Inc., "Data acquisition and control handbook," 2001.
[45] Texas Instruments, "A basic guide to thermocouple measurements," Report SBAA274, 2018.

Ferran Reverter was born in Llagostera, Spain, in 1976. He received the B.Sc. degree in industrial electronic engineering from the University of Girona, Girona, Spain, in 1998, the M.Sc. degree in electronic engineering from the University of Barcelona, Barcelona, Spain, in 2001, and the Ph.D. degree in electronic engineering from the Universitat Politècnica de Catalunya (UPC), Barcelona, Spain, in 2004.

Since 2001, he has been with the UPC, where he is an Associate Professor in Analog Electronics and Digital Systems. Since 2018, he has also been with the Open University of Catalonia, where he is a Course Instructor in Electronic Instrumentation. He was a visiting Post-Doctoral Researcher with the Delft University of Technology, Delft, The Netherlands from 2005 to 2007, and with the Imperial College London, London, U.K., in 2012. His current research interests include interface electronics for smart sensors, power-processing circuits for autonomous sensors, and MOSFET thermal sensors for IC testing.

He was awarded "Outstanding Reviewer" from the IEEE Instrumentation and Measurement Society three times (2014, 2018, and 2019). He is an Associate Editor of the IEEE Sensors Journal and IEEE Transactions on Instrumentation and Measurement.